



# Effect of the initial phase constitution in the low-cycle fatigue of NiTi wires

Jéssica Dornelas Silva<sup>1</sup>  · Vicente Tadeu Lopes Buono<sup>1</sup> Received: 11 June 2019 / Accepted: 8 November 2019 / Published online: 11 November 2019  
© Springer Nature Switzerland AG 2019

## Abstract

Vastly used due to their functional properties, NiTi shape memory alloys have mechanical properties and fatigue resistance known to be strongly affected by their thermomechanical state. In this work, the goal was to evaluate the fatigue resistance of near equiatomic Ni-rich NiTi heat treated wires in different tests temperature. In this manner, it was possible to evaluate the phase constitution effect on the fatigue resistance with a fixed thermomechanical condition. For that, a heat treatment at 500 °C for 30 min was performed in initially superelastic wires in an argon atmosphere. DSC tests were performed in order to obtain the transformation temperatures and there different fatigue test temperatures were chosen according to the phase stability ranges. Rotating-bending fatigue tests took place in proper equipment at 4% maximum strain, evaluating the properties of structures constituted by the R-phase, austenite and R-phase + austenite, in each selected test temperature. The results showed that the R-phase presents higher low-cycle fatigue resistance than austenite and a fatigue mechanism was proposed.

**Keywords** Nickel-titanium alloys · Shape memory · Superelasticity · Phase constitution · Fatigue resistance

## 1 Introduction

Near equiatomic NiTi alloys are attractive shape memory alloys due to the combination of their mechanical properties with their functional capabilities, being suitable to a wide range of engineering and medical applications [1]. Within these applications, NiTi wires are commonly subjected to substantial fluctuating stresses and strains, being prone to failure by fatigue. In cyclic conditions, NiTi wires can fail by functional fatigue, i.e., by losing their functional properties with an increasing number of cycles or by structural fatigue, i.e, damage accumulation during cyclic loading [2, 3]. The fatigue resistance of these alloys depends on the microstructure, the transformation temperatures and on the thermomechanical state. However, its complex structure and structure variations with the heat treatment

parameters and the thermomechanical history make fatigue behavior hard to understand and to predict [4–7].

In this context, recent studies have been made to evaluate some microstructural effects on the crack growth and fatigue life such as the effect of downsizing inclusions [8], grain size [9] and grain orientation around stress concentrators [10] as well as attempts to obtain analytical models to describe the non-linear fatigue behavior of these materials [11, 12]. Previous works by these authors [13, 14] have studied the effect of heat-treatments in different temperatures in a commercially available superelastic wire and it has been observed that the ones that promote precipitation of coherent  $Ti_3Ni_4$  particles and the formation of the R-phase in the working temperature provide good fatigue resistance in low-cycle fatigue. However, during a heat-treatment, other microstructural changes can take

✉ Jéssica Dornelas Silva, [jdornelassilva@gmail.com](mailto:jdornelassilva@gmail.com); [jdornelas@ufmg.br](mailto:jdornelas@ufmg.br); Vicente Tadeu Lopes Buono, [vbueno@demet.ufmg.br](mailto:vbueno@demet.ufmg.br) |

<sup>1</sup>Department of Metallurgical and Materials Engineering, Universidade Federal de Minas Gerais (UFMG), Av. Pres. Antônio Carlos, 6627 - Escola Engenharia - Bl. 2/sala 2246, 31270-901 Belo Horizonte, MG, Brazil.



place such as recovery and recrystallization processes, modifying the thermomechanical state of wires treated in different temperatures. In this manner, in the present study, the goal is to evaluate the effect of the different initial phases on the fatigue NiTi wires with a fixed thermomechanical history and the same surface condition, evaluating the effect of the present phases during cycling. For this purpose, fatigue tests were performed at different temperatures for wires with the same initial condition.

## 2 Materials and methods

The material used in this study was a 1 mm diameter 51 at% Ni–49 at% Ti commercially available superelastic wire heat-treated at 500 °C in a tubular furnace with an argon controlled-atmosphere for 30 min and then water cooled. The superelastic wire is drawn and pickled in its initial state, being in a strain-hardened condition, as previously noted in Ref. [14].

The heat-treated wires were firstly characterized at 22 °C by means of X-ray diffractometry (XRD) analyses and tensile tests from the water cooled samples. Hence, the obtained properties refer to a microstructure obtained by cooling from high temperatures. The XRD tests were performed for phase identification using Cu-K $\alpha$  ( $\lambda = 0.15418$  nm) radiation and a scan speed of 0.02/s. The peaks were identified by comparison with patterns from the ICSD database and spectra available in the literature [15–18].

The tensile tests took place in an Instron 5582 testing machine in order to evaluate the mechanical behavior of the wires. In accordance to ASTM F2516–14 standard [19], tests until rupture were performed at a crosshead speed of 12 mm/min and, in a different specimen, loading and unloading up to 6% deformation at a crosshead speed of 1.2 mm/min. The tested specimens presented useful lengths of 60 mm, resulting in strain rates of  $3.33 \times 10^{-3} \text{ s}^{-1}$  and  $3.33 \times 10^{-4} \text{ s}^{-1}$  for the rupture and loading/unloading tests respectively. The experiments were repeated three times and the strains were determined via mechanical extensometer.

Differential scanning calorimetry was performed to determinate the direct and reverse martensitic transformation temperatures and, thus, the phase stability range, in a Shimadzu DSC-60 calorimeter at a cooling/heating rate of 10 °C from –100 to 100 °C. The tests were performed in triplicate by cooling each specimen from room temperature to –100 °C, following by heating to 100 °C, cooling it back to –100 °C and heating to room temperature. The reverse transformation temperatures were determined in the interval from –100 to 100 °C, while the direct ones on the subsequent cooling step.

Then, the fatigue test temperatures were selected to evaluate the wire's performance with different phases. It is worth pointing out that the wires had the same surface condition, constituted by a thin layer of oxide resultant from the heat-treatment that could be observed by a surface coloring distinct from the wires in the initial condition, but it was not detected on the XRD analyses. The fatigue tests took place in proper flexural fatigue machine (Fig. 1) at 4% maximum strain in water baths at the chosen temperatures. During these rotating-bending fatigue test, the stress state changes continually along the wire's diameter, reaching maximum compression strains in the interior of the arc and maximum tensions strains at the exterior of the arc, similarly to other fatigue test apparatus present in the literature [20, 21].

The fractured surfaces of the samples subjected to the fatigue tests were analyzed in an FEI—inspect 550 scanning electron microscope (SEM) operating at 15 kV using secondary electrons. Additionally, the longitudinal sections of the samples fractured in one-phase regions (10 °C and 55 °C) were polished and analyzed in the SEM unetched.

## 3 Results

The diffractogram obtained for the heat-treated wires at room temperature (XRD) indicates the presence of the R-phase and of austenite. The R-phase was identified, as it can be seen in Fig. 2 [15, 22, 23]. However, the R-phase peak splitting is not well defined, as it is exemplified in Fig. 2b. This is an indication that austenite is also present at this temperature. The presence of precipitates Ti<sub>3</sub>Ni<sub>4</sub> could also be noted [24].

The mechanical behavior of the specimens in the tensile tests is presented in Fig. 3. In the rupture curve, represented as a full line, the stress plateau was reached at



Fig. 1 Rotating-bending fatigue test apparatus

**Fig. 2** Characteristic R-phase peaks observed in the XRD analysis of the heat-treated alloy at room temperature

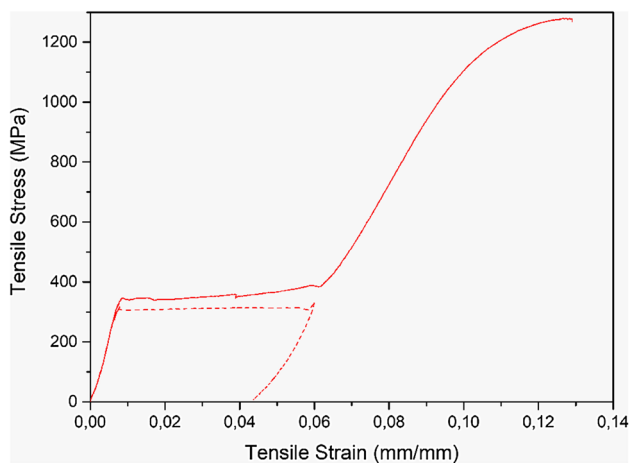
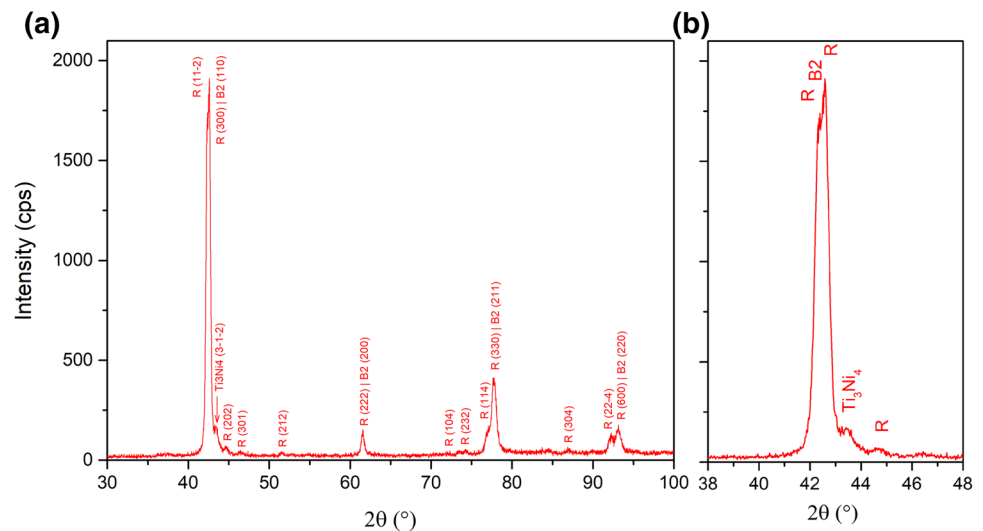


**Fig. 3** Representative tensile stress  $\times$  strain rupture (full line) and loading/unloading curves (dashed line) obtained in the tension test of the heat-treated sample at room temperature

around 350 MPa with a corresponding maximum strain of around 6%. A mean rupture stress of 1280 MPa was observed with a deviation smaller than 2% and an apparent Young Modulus of 48 GPa was obtained. In the loading/unloading curve, represented as a dashed line, the stress at which the plateau is reached is around 300 MPa. The difference between the value obtained from the rupture curve and the loading/unloading curve can be explained by the different strain rates used in each test. Moreover, a large residual strain was observed during unloading and a full shape recovery could be achieved by heating.

Figure 4 presents the obtained DSC chart. Two peaks were detected during cooling and during heating, characterizing a symmetric R-phase transformation [25]. Martensitic transformations involving the R-phase are common on heat-treated samples. The R-phase is a pre-martensitic

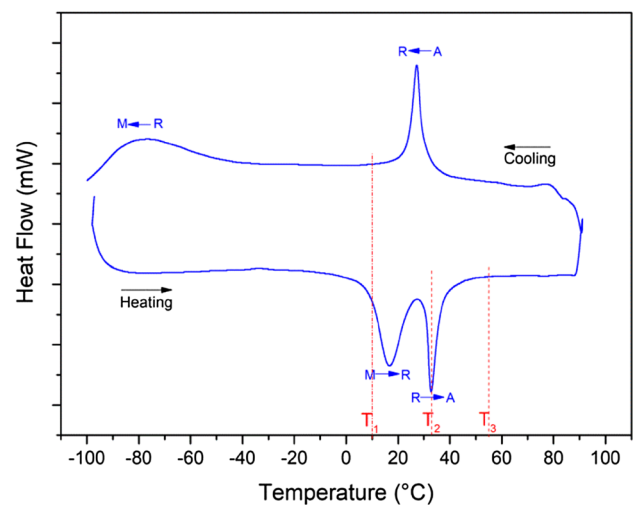


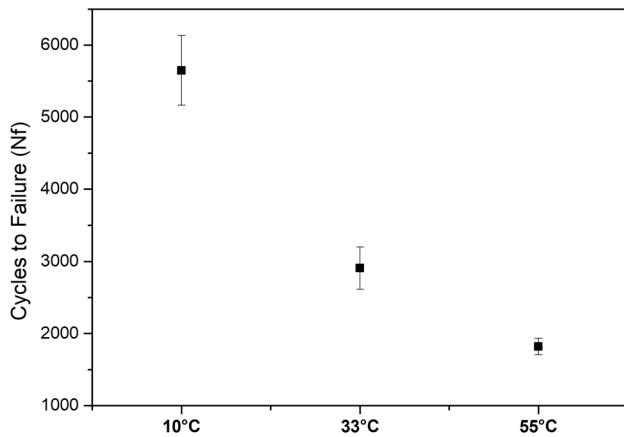
**Fig. 4** DSC chart obtained for the heat treated wire, where the selected fatigue test temperatures  $T_1$ ,  $T_2$  and  $T_3$  are highlighted

trigonal phase that involves transformation lattices distortions much smaller than the martensitic direct transformations. Coherent precipitates formed during heat-treatments generate lattice distortions that favor the R-phase formation and, thus, two-step transformations [26]. Hence, the formation of coherent  $Ti_3Ni_4$  particles can be inferred, in accordance to the observed XRD  $Ti_3Ni_4$  peak.

In this manner, the detected DSC peaks are identified on the chart in accordance to Refs. [14, 17, 25, 27]. During cooling, the first peak refers to austenite (A)  $\rightarrow$  R-phase (R) transformation and the second to the R-phase (R)  $\rightarrow$  martensite (M) transformation. During heating, the first peak refers to an M  $\rightarrow$  R transformation and the second, to an R  $\rightarrow$  A transformation. Note that there is a small hysteresis between the R  $\leftrightarrow$  A transformations during cooling and

**Table 1** Temperatures selected after de DSC analyses for the fatigue test and the respective inferred phase constitution

	Temperature	Phase constitution in stress free condition
T <sub>1</sub>	10 °C	R-phase
T <sub>2</sub>	33 °C	R-phase + austenite
T <sub>3</sub>	55 °C	Austenite

**Fig. 5** Mean number of cycles to failure at 4% maximum strain rotating-bending fatigue tests in each test temperature

heating and that these peaks have a characteristic sharp profile like pointed out by Wang [17].

Considering the heat-treated wires are kept at room temperature (~22 °C), three different temperatures were selected to perform the fatigue tests and are presented in Table 1. T<sub>1</sub> is in a region where the R-phase is predominant on the cooling curve, which can be obtained by cooling the heat-treated samples. T<sub>3</sub> is in an austenitic region and T<sub>2</sub>, in a two-phase austenitic + R-phase region on the heating curve, since both of these temperatures are above room temperature and can be obtained by heating the heat-treated samples.

The mean numbers of cycles to failure in each temperature are presented in Fig. 5. The highest fatigue life was observed on the structure initially constituted by the R-phase (10 °C) and the lowest, on the austenite (55 °C). The initially two-phase structure at 33 °C presented an intermediate behavior.

The fracture surfaces of the fatigue tested samples (Fig. 6) presented two different regions: a slow fatigue crack propagation region (region 1 in Fig. 6) and a ductile final rupture region (region 3 in Fig. 6). Between these two regions, a transition zone can be observed, identified as the region 2. While the crack nucleation and slow propagation region, shown in detail in Fig. 5b, e, h, is characterized

by the presence of fatigue striations, the ductile fracture region, shown in Fig. 5c, f, i, is characterized by the presence of dimples. It is possible to notice in Fig. 5 (a, d and g) that the area corresponding to the final ductile fracture is larger in the sample initially constituted by austenite (55 °C) in such way that the slow crack propagation region is larger in samples initially constituted by the R-phase. Also, multiple crack nucleation sites could be observed, as there were multiple secondary slow crack propagation regions, delimited in region 3.

It is worth noting that microcracks could be observed through the striations in the slow propagation area of the samples tested at 33 °C and 55 °C, as it can be noted in Fig. 7. These types of microcracks were not observed in the samples tested at 10 °C.

In the longitudinal sections of the samples, transverse cracks were observed along the length of the fractured wires. The longest cracks found in the samples tested at 10 °C and 55 °C are illustrated in Fig. 8. It is possible to note that the cracks are longer in the sample tested at 10 °C than in sample tested at 55 °C.

## 4 Discussion

The highest number of cycles to failure was obtained at 10 °C, in the initially R-phase structure and the lowest at 55 °C, in the initially austenitic structure. The samples with an initially dual-phase structure presented intermediate fatigue resistance. These results are in agreement with previous tests at 4 °C for samples heat-treated in different conditions [14]: the samples initially constituted by the R-phase presented much higher fatigue resistance at 4% strain than an initially austenitic structure.

While in the studies performed in Ref. [14], the samples with different microstructures were obtained by heat-treatment in different temperatures—and hence, having different thermic histories, in this study the different initial microstructures were obtained by using different test temperatures. In such case, the effect of the test temperature must also be considered.

In shape memory alloys, besides determining the phase constitution, the working/testing temperature may also have effects in the fatigue mechanisms. In fact, it has been previously observed [28] that the unrecovered strains and plastic deformation increase exponentially with increasing temperature in superelastic wires.

During cycling in a fatigue regime, cracks nucleate on stress concentration regions and go through a process of growing and blunting up until a point where the predominant crack reaches a critical size and propagates unstably, causing the component's fracture. In high stress/strain amplitudes, the crack propagation is an essential aspect



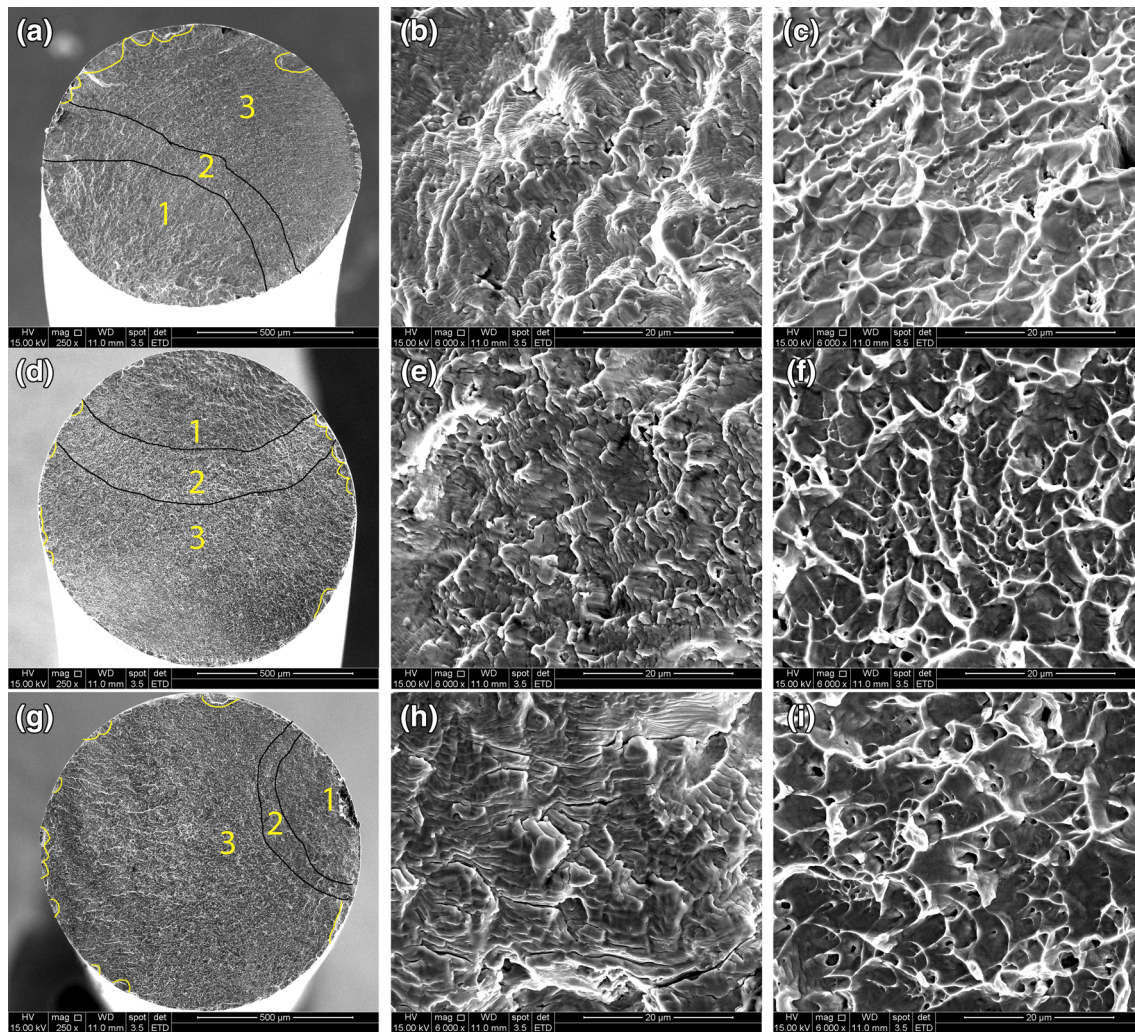


**Fig. 6** Fracture analysis of samples tested in fatigue at **a–c** 10 °C; **d–f** 33 °C; and **g–i** 55 °C

of the fatigue resistance, since it prevails in low-cycle fatigue in NiTi alloys, as reported in the literature [29–32]. The aggressive strain amplitude applied to the wires favors fast crack nucleation, as it can be related to the various fatigue initiation sites along the fracture surfaces in Fig. 6, making crack propagation predominant on the fatigue life.

Since the majority of the fatigue life is related to crack propagation and samples initially constituted by the R-phase presented the highest number of cycles to failure, it can be assumed that crack propagation in this situation requires amounts of energy higher than at an initially austenitic structure, resulting in slower propagation and higher number of cycles to failure. The smaller fraction of ductile fracture area in the sample tested at 10 °C fractography and apparent smaller striation spacing are evidence of the statement above. Additionally, the presence of longer cracks in the longitudinal section of the initially R-phase structure can also be related to the longer time

required to propagate the predominant crack, giving time for secondary cracks in other planes to grow. Besides, the longer size of this cracks when compared to the initially austenitic wires could be an indication that this structure bares longer cracks.

Unlike in conventional materials, the crack propagation in low-cycle fatigue of NiTi seems to be deeply related to the martensitic induced transformation rather than by the existence of a plastic region around the crack tip [33, 34]. In both microstructures, the induced martensitic transformation is expected to occur during loading on cycling, but while the reverse transformation occurs during unloading in the austenite, it probably does not occur in the R-phase, as it was observed in the tensile tests at room temperature in Fig. 3. This observation is endorsed by previous studies [13, 14], where it was observed that the R-phase does not undergo significant reverse transformation at room temperature. Additionally, it is worth pointing out that it



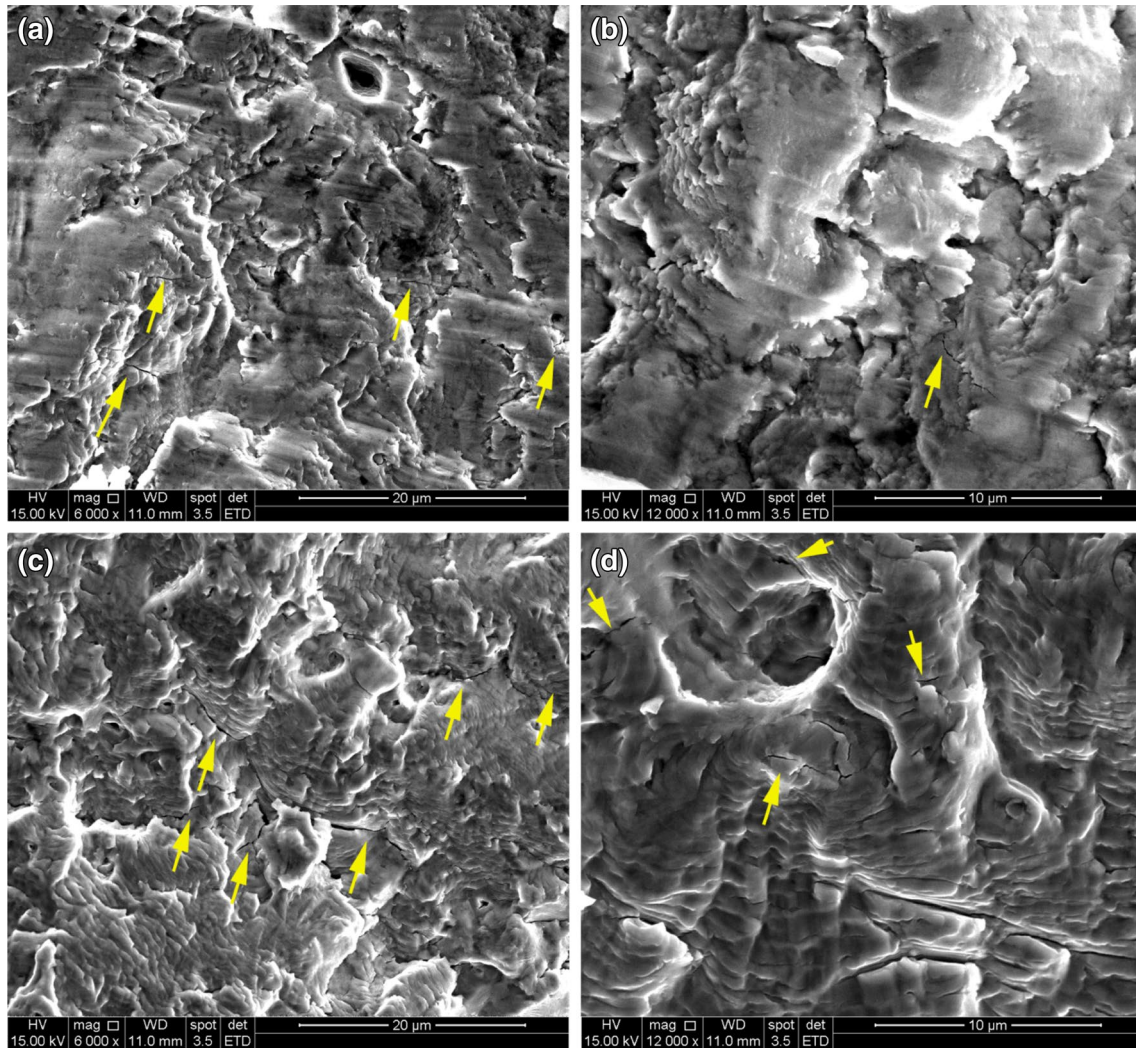


Fig. 7 Microcracks observed in the slow crack propagation region in samples tested at **a, b** 33 °C and **c, d** 55 °C

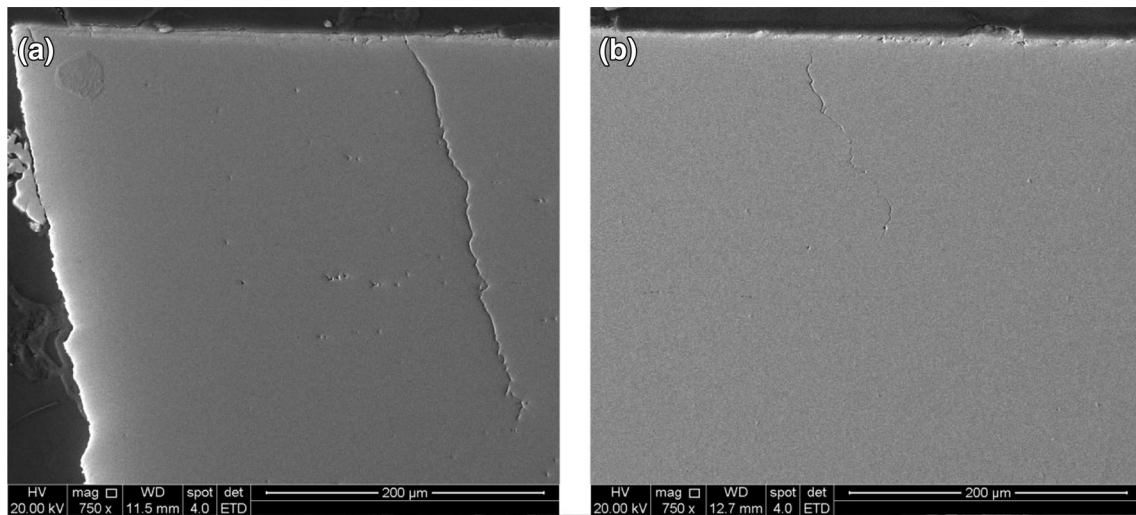


Fig. 8 Polished longitudinal section of wires tested and fractured at **a** 10 °C, in the R-phase region and at **b** 55 °C, in the austenitic region

has been observed that biphasic structures tested in tension at 37 °C presented significant shape recovery through reverse transformation.

Hence, to propose a fatigue mechanism, it can be assumed that the initially R-phase structure goes through an induced martensitic transformation, which in turn occurs in tensions lower than the ones required to induce this transformation in the austenitic wires in higher test temperatures. The biphasic structure can be assumed to undergo induced transformation and partial reverse transformation. The austenitic structure can be assumed to undergo elastic and reverse martensitic transformation.

On the one hand, the induced martensitic transformation from austenite is reported [28, 35, 36] to be associated with a high amount of generated dislocations. The high amount of microcracks through the striations in the samples tested at 55 °C and 33 °C (Figs. 5h, 6) can be related to a local stress concentration due to the dislocations generated during the induced and reverse martensitic transformation. Besides, the high test temperature can be related to high amounts of unrecovered strains, as it has been observed by [28]. This fact can also be an explanation for why there is a higher amount of microcracks in samples tested at 55 °C than at 33 °C.

On the other hand, while in the initially austenitic structure cracks propagate generating a high amount of defects on the crack tip and where stress-induced martensitic transformation occurs, in the R-phase, where martensite is formed in the regions of maximum strain amplitudes and around cracks nucleated along the wire, the martensitic structure is the predominant phase in these regions and it is the main phase that bears the fatigue damage accumulation. In this case, it has been previously stated [7] that on the R-phase/martensite structure, the variant interfaces give the crack multiple paths to propagate, inducing crack branching with high energy dispersion. This can be the reason why fine striation spacing is observed in the fractured surface of the specimens with the initial R-phase structure, indicating that small increments on the fatigue crack size take place during cycling.

Additionally, while the wire in the austenitic state is expected to present superelastic behavior, in wires in the R-phase/martensitic structure, it is expected that the martensite undergoes cyclic reorientation during cycling. In this manner, the tensions involved during cycling in the initially austenitic state are expected to be higher than in the initially R-phase state. This can also be a contributing factor to the lowest fatigue life observed at 55 °C.

In summary, the results of this study showed that the relative fatigue slow propagation area is larger in the R-phase initial condition, as compared to the initially austenitic. It was also observed that the longitudinal

section of wires tested in the R-phase region presented longer cracks along the wire transverse section than in wires tested in the austenitic region. These results lead to the conclusion that in an initially R-phase structure, there is high energy dispersion during propagation when compared to the austenite.

To explain this behavior, it is proposed that, during cycling, the austenite presents superelastic behavior while the R-phase transforms into martensite, which in turn undergoes cyclic reorientation. Besides that, the stress-induced and reverse martensitic transformations are reported to be associated with a high amount of generated defects along with the occurrence of localized plastic deformation due to the high test temperature, while in the initially R-phase structure, lower stresses are involved during cycling, related to martensitic reorientation.

## 5 Conclusions

In this paper, bending-rotating fatigue tests at 4% maximum strain amplitude were performed at 10 °C, 33 °C and 55 °C in NiTi heat-treated wires. At 10 °C, the wires should be initially constituted by the R-phase, at 33 °C by a dual-phase austenite + R-phase, and at 55 °C by austenite. The highest number of cycles to failure was obtained in the R-phase structure. This result can be related to the fact that, during cycling, the R-phase/martensitic structure undergoes martensitic reorientation and the cracks propagate with high energy dispersion. In the austenitic structure, on the other hand, a high amount of defects associated with the stress-induced martensitic and reverse transformations during cycling is expected to be generated, hindering its fatigue resistance when compared to the initial R-phase state. Additionally, the presence of different phases in different test/working temperature may be the explanation for the decrease in the fatigue life with increasing temperature in the low-cycle fatigue life of NiTi along with the increase of localized plastic deformation with temperature.

**Acknowledgements** This study was partially financed by the Coordenação de Aperfeiçoamento de Pessoal de Nível Superior - Brasil (CAPES) - Finance Code 001, Conselho Nacional de Desenvolvimento Científico e Tecnológico (CNPq) and the Fundação de Amparo à Pesquisa de Minas Gerais (FAPEMIG).

## Compliance with ethical standards

**Conflict of interest** The authors state that there are no conflicts of interest in this paper.

## References

- Otsuka K, Wayman CM (1998) Shape memory materials. Cambridge University Press, Cambridge
- Oliveira JP, Miranda RM, Schell N, Fernandes FMB (2016) High strain and long duration cycling behavior of laser welded NiTi sheets. *Int J Fatigue* 83:195–200. <https://doi.org/10.1016/j.ijfatigue.2015.10.013>
- Eggeler G, Hornbogen E, Yawny A et al (2004) Structural and functional fatigue of NiTi shape memory alloys. *Mater Sci Eng A* 378:24–33. <https://doi.org/10.1016/j.msea.2003.10.327>
- Kollerov M, Lukina E, Gusev D et al (2013) Impact of material structure on the fatigue behaviour of NiTi leading to a modified Coffin-Manson equation. *Mater Sci Eng A* 585:356–362. <https://doi.org/10.1016/j.msea.2013.07.072>
- Pelton AR (2011) Nitinol fatigue: a review of microstructures and mechanisms. *J Mater Eng Perform* 20:613–617. <https://doi.org/10.1007/s11665-011-9864-9>
- Khalil-allafi J, Eggeler G, Dlouhy A et al (2004) On the influence of heterogeneous precipitation on martensitic transformations in a Ni-rich NiTi shape memory alloy. *Mater Sci Eng A* 378:148–151. <https://doi.org/10.1016/j.msea.2003.10.335>
- Figueiredo AM, Modenesi P, Buono V (2009) Low-cycle fatigue life of superelastic NiTi wires. *Int J Fatigue* 31:751–758. <https://doi.org/10.1016/j.ijfatigue.2008.03.014>
- Coda A, Cadelli A, Zanella M, Fumagalli L (2018) Straightforward downsizing of inclusions in NiTi alloys: a new generation of SMA wires with outstanding fatigue life. *Shape Mem Superelasticity* 4:41–47. <https://doi.org/10.1007/s40830-018-0159-y>
- Lepage WS, Ahadi A, Lenthe WC et al (2018) Grain size effects on NiTi shape memory alloy fatigue crack growth. *J Mater Res* 33:91–107. <https://doi.org/10.1557/jmr.2017.395>
- Paul PP, Fortman M, Paranjape HM et al (2018) Influence of structure and microstructure on deformation localization and crack growth in NiTi shape memory alloys. *Shape Mem Superelasticity*. <https://doi.org/10.1007/s40830-018-0172-1>
- Allegretti D, Francesca Berti B, Francesco Migliavacca B et al (2018) Fatigue assessment of nickel–titanium peripheral stents: comparison of multi-axial fatigue models. *Shape Mem Superelasticity* 4:186–196. <https://doi.org/10.1007/s40830-018-0150-7>
- Vantadori S, Carpinteri A, Di Cocco V et al (2018) Fatigue analysis of a near-equiatomic pseudo-elastic NiTi SMA. *Theor Appl Fract Mech* 94:110–119. <https://doi.org/10.1016/j.tafmec.2018.01.012>
- Dornelas J, Damas P, Ribeiro P et al (2019) Fatigue resistance of dual-phase NiTi wires at different maximum strain amplitudes. *Int J Fatigue* 125:97–100. <https://doi.org/10.1016/j.ijfatigue.2019.03.040>
- Dornelas J, Martins SC, Lopes N et al (2019) Effects of aging treatments on the fatigue resistance of superelastic NiTi wires. *Mater Sci Eng A* 756:54–60. <https://doi.org/10.1016/j.msea.2019.04.037>
- Santos LDA, Resende PD, Bahia MGDA, Buono VTL (2016) Effects of R-phase on mechanical responses of a nickel–titanium endodontic instrument: structural characterization and finite element analysis. *Sci World J*. <https://doi.org/10.1155/2016/7617493>
- Kim JI, Liu Y, Miyazaki S (2004) Ageing-induced two-stage R-phase transformation in Ti 50.9 at% Ni. *Acta Mater* 52:487–499. <https://doi.org/10.1016/j.actamat.2003.09.032>
- Wang XB, Verlinden B, Van Humbeeck J (2014) R-phase transformation in NiTi alloys. *Mater Sci Technol* 30:1517–1529. <https://doi.org/10.1179/1743284714Y.0000000590>
- Sinha A, Mondal B, Chattopadhyay PP (2013) Mechanical properties of Ti-(~49 at%) Ni shape memory alloy, part II: effect of ageing treatment. *Mater Sci Eng A* 561:344–351. <https://doi.org/10.1016/j.msea.2012.10.023>
- (2015) Standard test method for tension testing of nickel–titanium superelastic materials. ASTM - F2516 1–6
- Oliveira JP, Fernandes FMB, Schell N, Miranda RM (2015) Shape memory effect of laser welded NiTi plates. *Funct Mater Lett* 8:1–5. <https://doi.org/10.1142/S1793604715500691>
- Tobushi H, Hachisuka T, Yamada S, Linc P (1997) Rotating-bending fatigue of a TiNi shape-memory alloy wire. *Mech Mater* 26:35–42
- Mohri M, Taghizadeh M, Wang D et al (2018) Microstructural study and simulation of intrinsic two-way shape memory behavior of functionally graded Ni-rich/NiTiCu thin film. *Mater Charact* 135:317–324. <https://doi.org/10.1016/j.matchar.2017.11.056>
- Sittner P, Landa M, Lukás P, Novák P (2006) R-phase transformation phenomena in thermomechanically loaded NiTi polycrystals. *Mech Mater* 38:475–492. <https://doi.org/10.1016/j.mechmat.2005.05.025>
- Prokofiev EA, Burrow JA, Payton EJ et al (2010) Suppression of Ni<sub>4</sub>Ti<sub>3</sub> precipitation by grain size refinement in Ni-rich NiTi shape memory alloys. *Adv Eng Mater* 12:747–753. <https://doi.org/10.1002/adem.201000101>
- Duerig TW, Bhattacharya K (2015) The influence of the R-phase on the superelastic behavior of NiTi. *Shape Mem Superelasticity* 1:153–161. <https://doi.org/10.1007/s40830-015-0013-4>
- Otsuka K, Ren X (2005) Physical metallurgy of Ti–Ni-based shape memory alloys. *Prog Mater Sci* 50:511–678. <https://doi.org/10.1016/j.pmatsci.2004.10.001>
- Tan L, Crone WC (2004) In situ TEM observation of two-step martensitic transformation in aged NiTi shape memory alloy. *Scr Mater* 50:819–823. <https://doi.org/10.1016/j.scriptamat.2003.12.019>
- Heller L, Seiner H, Sittner P et al (2018) On the plastic deformation accompanying cyclic martensitic transformation in thermomechanically loaded NiTi. *Int J Plast*. <https://doi.org/10.1016/j.iijplas.2018.07.007>
- Fine ME, Chung Y-W (1996) Fatigue failure in metals. In: ASM handbook—fatigue and fracture. ASM International
- Bahia MGA, Gonzalez BM, Buono VTL (2006) Fatigue behaviour of nickel–titanium superelastic wires and endodontic instruments. *Fatigue Fract Eng Mater Struct* 29:518–523. <https://doi.org/10.1111/j.1460-2695.2006.01021.x>
- Robertson SW, Pelton AR, Ritchie RO (2012) Mechanical fatigue and fracture of Nitinol. *Int Mater Rev* 57:1–37. <https://doi.org/10.1179/1743280411Y.0000000009>
- Sawaguchi T, Kaustrater G, Yawny A, Wagner M (2003) Crack initiation and propagation in 50.9 at% Ni–Ti pseudoelastic shape-memory wires in bending-rotation fatigue. *Metall Mater Trans A* 34:2847–2860
- Di Cocco V, Iacoviello F, Maletta C, Natali S (2014) Cyclic microstructural transitions and fracture micromechanisms in a near equiatomic NiTi alloy. *Int J Fatigue* 58:136–143. <https://doi.org/10.1016/j.ijfatigue.2013.03.009>
- Gollerthan S, Young ML, Baruj A et al (2009) Fracture mechanics and microstructure in NiTi shape memory alloys. *Acta Mater* 57:1015–1025. <https://doi.org/10.1016/j.actamat.2008.10.055>
- Delville R, Malard B, Pilch J et al (2011) Transmission electron microscopy investigation of dislocation slip during superelastic cycling of Ni–Ti wires. *Int J Plast* 27:282–297. <https://doi.org/10.1016/j.iijplas.2010.05.005>
- Alarcon E, Heller L, Chirani SA et al (2017) Fatigue performance of superelastic NiTi near stress-induced martensitic transformation. *Int J Fatigue* 95:76–89. <https://doi.org/10.1016/j.ijfatigue.2016.10.005>

**Publisher's Note** Springer Nature remains neutral with regard to jurisdictional claims in published maps and institutional affiliations.